

## **Modelling of Combustion in Rocket Engines using Pintle Injectors**

Gurunadh Velidi \*, Divyam Paliwal, Prashant Gahlot, Suramya Bhatt and Vanshika

Department of Aerospace Engineering  
University of Petroleum and Energy Studies  
Dehradun, India

### **Abstract**

While developing a rocket engine, combustion instabilities have posed a major challenge which is in turn dependent on the design of an injector and, thus a topic of research among various engineers and researchers. In this paper, we have worked on an injector that can control both injection area and velocity and able to maintain good spray conditions at low mass flow rates of propellants unlike conventional injectors with the fixed areas. The injector of such kind was invented in the mid-1950s in Jet Propulsion Laboratory for the Apollo missions to achieve controllable combustion. The main function of the injector is to take the propellant and ensure that it is mixed properly so that the combustion is as complete as possible before exhaust. Keeping a note of these requirements, some of the injector parameters were varied and a study on the variation of Sauter mean diameter, velocity profile, and optimization of the combustion efficiency is done. Variation of Sauter means diameter was determined by experimental values. The diameter decreases as Weber's number increases by making distribution more uniform and its distribution is important for ignition stability, combustion efficiency, and for engine thermal protection whereas Velocity profile, using steady and 2D axisymmetric conditions. Eddy-dissipation concept model with 6-Step Jones-Lindstedt mechanism was used for the turbulent reaction. Various sets of the combination of pintle-tip angle and pintle opening distance are selected and the study of the effect of these parameters on the injecting propellant are observed. Also, since the properties of the propellants also hold some significance, the optimum propellant combination will be found by studying the properties of propellants using appropriate software.

---

\*Corresponding Author: guru.velidi@gmail.com

## Introduction

The Pintle injector is a re-attracted injection mechanism for a liquid rocket engine that has many advantages, including the use of a single injector assembly over several injector components and wide throttle ability with high performance. Because of these benefits, the pintle injector is the most commonly used injector in today's liquid rocket engines by Space X and Northrop Grumman Aerospace Systems with various features of throttling, rapid pulsing capability, and face shut off. Pintle injector differs from traditional injector in terms of its basic construction, strong variable-condition adaptability, and robust combustion [4]. The Apollo lunar descent engine (thrust ratio 10: 1) [11], the main engine of the Chang'e-3 lunar probe spacecraft (thrust ratio 5: 1) [13], and the Merlin 1D engine of the Falcon 9 rocket (thrust ratio 2: 1) [12] are few of the Pintle injector's effective applications which have helped in providing an efficient solution for combustion instabilities. Pintle injectors have gone through three stages of growth: linear modification, low temperature, and no toxicity, over the course of decades of development [14]. As a result, Pintle injectors are best suited for LOX/GCH<sub>4</sub> variable-thrust rocket engines which have significant scientific implications and a wide range of potential applications.

Propulsion system is the heart of the rocket engine and injector being the major part affects its performance. In 1962, Rocket dyne was ready to test the engine of F1 but as the engine ignited and turbo-prop spooled up, the test failed because the engine exploded and the reason behind this catastrophic disaster is combustion instability. Chugging is a type of low frequency instability which occurs due to the variation in the mass flow rates of both oxidizer and fuel as a result pressure drop occurs across the injector and thus, results in cyclic thrust variations. However, if the frequency range reaches the intermediary stage of 400- 1000 Hz it is termed as buzzing. These combustion instabilities are capable of damaging the thrust chamber, throat and structure, unchecked impulse and thrust variation. Therefore, to fulfill these requirements, combustion chamber length should be small and there should not be any hot spots present which means combustion temperature is within limits. Injector design plays a major role in controlling the combustion instabilities.

There are various types of injectors depending on the requirements of the rocket thrust.

1. Shower Head type
2. Self-Impinging doublet type
3. Cross impinging triplet type

## 4. Centrifugal or Swirling type

## 5. Pintle injector type

Showerhead type is the most basic injector design but it has poor atomization and leads to large combustion chamber volume. All other types are an advanced version of later injectors.

Recent research on Pintle injectors show that larger values of Pintle angle have more stable flow when compared to smaller values. Dr.R.Rajendran Prasad et al. in their research showed how parameters like Spray angle and Sauter mean diameter affects the performance of Pintle injector by taking two different Pintle angles i.e. 20 and 33 degree respectively and calculating various parameters like TMR, Weber number, spray angle. [8] A. Frassoldati in their research mentioned various mechanisms to describe the combustion of methane and to study oxy-fuel conditions. Experimental data corresponding to the required set of contour flow diffusion flames is selected and the optimized mechanism was applied with methane and oxygen. The results showed improvement in numerical values when compared to the original mechanism. [7] Son, in their study, compared the results from experimental and actual simulation to verify the spray characteristics study of Pintle injector. From the above results, they have concluded that the values of gas velocities are nearly the same at maximum and minimum points and there is a difference in velocity profile for a simulated and measured profile. Research is done on recirculation zones and spray density distribution as shown in the paper. [3]

From the literature review, investigation was done to decide the base geometry of the Pintle injector with specific dimensions for the benchmark study. The geometry of the Pintle injector used for this paper has been adopted from a research paper published by M. Son with three others in 2017. [1] Variations in the geometry was done and each case was analyzed for different values of pintle tip angle using ANSYS Fluent solver and CHEMKIN transport model. CHEMKIN reaction model uses multi-step reaction which more accurate to the real case. This paper contains the study of Pintle injector which has been selected as it can control the mass flow rate of propellants and their spray characteristics. This control is provided with the help of its unique geometry that provides a different flow field in the combustion chamber. Here, we focused on the proper mixing of propellants by varying Pintle centre post radius and varying Pintle angles to attain optimum results.

## Computational analysis and validation

**Domain:** Figure 1 depicts the two-dimensional configuration and computational domain of the GOX/LCH<sub>4</sub> pintle injector prototype. The geometry has been adopted from a research paper published by M. Son et al. in 2017. This model's throat diameter was 10 millimeters, and the combustion chamber's maximum length with the nozzle was 242 millimeters. The diameter and length of the cylindrical component were 60 mm and 66 mm, respectively. [1] To compare the distributions of species in the room, four axial points with a 20-mm interval were chosen based on the pintle tip end.

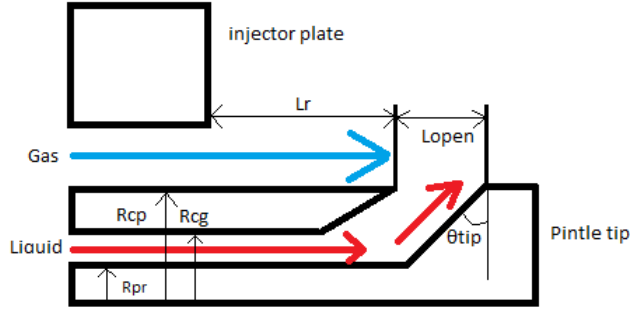


Figure 1. Schematic of a pintle injector

Center Gap Radius	$R_{cg}$	4.0
Center Gap Radius	$R_{cp}$	8.0
Pintle rod radius	$R_{pr}$	3.0
Pintle tip diameter	$D_{pt}$	12.0
Pintle opening distance	$L_{open}$	0.6
Pintle tip angle	$\theta_{pt}$	40

Table 1. Dimensions of a Pintle injector

The simulation was carried out using the industrial software programme FLUENT. Various equations for 2D axisymmetric geometries were used to measure the flow variables in the computational domain. The pressure-velocity coupled solver was used, and the spatial discretization was done using a second order upwind method. To research turbulent combustion, an eddy-dissipation theory model (EDC) was used. In the EDC, reaction rates were measured by generating small-scale eddies in a turbulent flow governed by turbulent kinetic energy (K) and turbulent dissipation energy. In general, the EDC estimates temperature and flame length by calculating the reaction rate for each reaction separately. Giorgi et al.

compared various forms of the coaxial rocket injector.[16]

They discovered that the EDC produced more accurate numerical results and was less expensive numerically than the probability density function form (PDF). Instead of using detailed full-step methods, a simpler Jones–Lindstedt 6-step system (JL6) with 6 equations and 9 species was used, as seen in Table 2. Giorgi compared experimental results to the simulation findings of rocket combustion using JL6. Second, Frassoldati et al. [17]

Reactions	A	B	Ea (cal/mole)
$\text{CH}_4 + 0.5 \text{O}_2 \Rightarrow \text{CO} + 2 \text{H}_2$ CH <sub>4</sub> /0.50 /O <sub>2</sub> /1.3/	3.6e10	0.0	30,000
$\text{CH}_4 + \text{H}_2\text{O} \Rightarrow \text{CO} + 3 \text{H}_2$	3.84e09	0.0	30,000
$\text{CO} + \text{H}_2\text{O} \rightleftharpoons \text{CO}_2 + \text{H}_2$	2.01e09	0.0	20,000
$\text{H}_2 + 0.5 \text{O}_2 \rightleftharpoons \text{H}_2\text{O}$ O <sub>2</sub> /0.3 /O <sub>2</sub> /1.55/	8.06e16	-1.0	40,000
$\text{O}_2 \rightleftharpoons 2 \text{O}$	1.05e09	0.0	113,000
$\text{H}_2\text{O} \rightleftharpoons \text{H} + \text{OH}$	2.30e22	-3.0	120,000

Figure 2. Jones-Lindstedt mechanism modified by Frassoldati

**Boundary Conditions:** Gaseous methane and oxygen were pumped into the central and annular spaces as fuel and oxidizer respectively at 300 K. A pressure-based solver was used for steady calculations, and a 2D axisymmetric state was assumed. The density was calculated using the ideal gas assumption, and a conventional K-epsilon model was used for turbulent modeling, with normal wall functions as the near-wall treatment. The adiabatic condition was assumed for the remaining walls, and the combustion chamber wall and nozzle boundary conditions were set to a constant temperature of 600 K. Chemkin 6 phase reaction produced by JL6 for oxy-fuel methane combustion. They contrasted the two-step and four-step processes of Westbrook and Dryer (WD) and Jones and Lindstedt (JL) and validated the numerical values of WD and JL in methane and oxygen combustion at oxy-fuel conditions with experimental values. After contrast, the JL process was improved to JL6.[16]

Several cases of different geometries, varying pintle centre post radius and pintle angle were considered for the simulations, as mentioned in the table below.

Case 1 is the basic case with the pintle angle fixed at 50 degree in the study by M. Son et al. in 2017, other cases have geometric variations. Keeping the centre post radius same but reducing the angle to 30 and comparing the results. Furthermore, the greater radii of centre posts in case 4, case 5 and case 6 could monitor the recirculation region near the pintle tip while also reducing injection velocity due to a larger annular injection field. For comparison, six different cases with two different center post radius and pintle tip angle were selected as mentioned in table. In order to study the variation of sauter mean diameter, case 2 and case 3 were compared at different pintle tip angle, keeping the center post radius same as case 1.



**Figure 3.** Pintle Injector Geometries

The effect of pintle post radius is determined by comparing case 2 and case 4, where the opening distance of the injector and the pintle tip angle were kept same but the center post radius were varied. Finally, for selecting the optimum design of the injector, different angles at 6mm center post radius were compared for achieving the most suitable Sauter mean diameter value.

	Center post radius (mm)	Pintle tip angle (deg)
Case 1	4	50
Case 2	4	30
Case 3	4	20
Case 4	6	30
Case 5	6	50
Case 6	6	40

**Table 2.** Dimensions of Major geometry variations

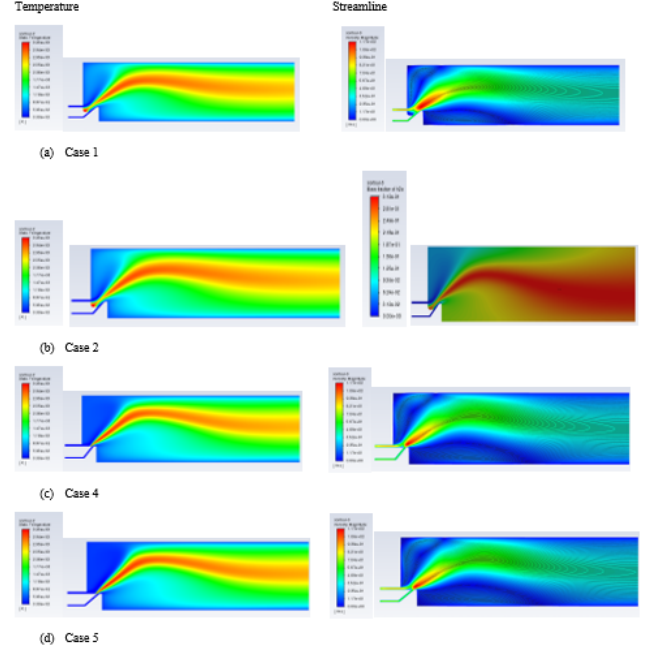


**Figure 4.** Numerical Contours and Streamline

**Meshing:** For the combustion analysis, the smallest number of mesh counts was considered in order to reduce computing capacity and time. The mesh was generated using the parameters mentioned above, and the mesh's final characteristic is as follows:

Mesh Parameter	Assigned Values
Mesh Sizing	0.00023
Edge Sizing	0.00023
Element method	Multi-Zone(All quad)
Constrain Parameter	Face Meshing
Mesh count	169695
Node count	170895
Orthogonal Quality	0.9998

**Table 3.** Mesh Sizing Parameters & Statistics

The mesh was controlled for the orthogonal quality so that there is consistency in the results of the analysis. The visualization of mesh as shown in figure 5.

The mesh must be checked against the data from the literature review, which serves as proof for the research conducted. The ANSYS Fluent simulation of propellant mixture CH<sub>4</sub>-LOX combustion in the Pintle single-injector by M. Son et al. was used to generate the simulation results. The study was

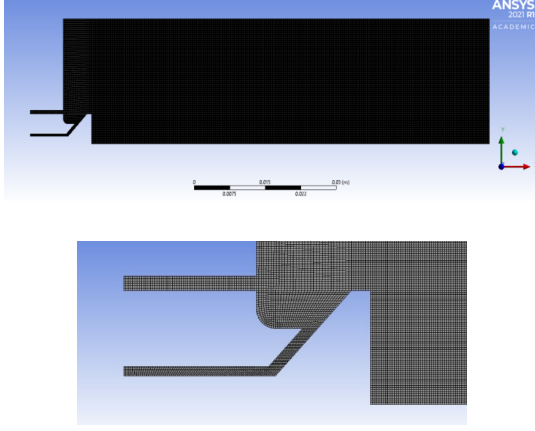


**Figure 5.** Mesh

carried out using the same boundary conditions as in the literature review, and the turbulence model used was k-epsilon, as in the literature review, as well as a bulk viscosity model with Eddy Dissipation (EDM) transport model. The simulation was run until the convergence conditions were met, which was 10-6.

The mesh needs to be validated with the data mentioned in the research paper published by M. Son, which is also the base paper for this project. The temperature of case 1(4mm center post radius, 40deg pintle angle), also the base case, was achieved between 300k to 3200k, also in the study done by M. Son et al. the temperature was between 300k to 3200k. Whereas the values of mass fraction of H<sub>2</sub>O and OH achieved by M. Son et al. are between 0 to 0.43, and 0 to 0.13 respectively. In our validation, values of mass fraction of H<sub>2</sub>O and OH were obtained from 0 to 0.312, and 0 to 0.141 respectively. The molar concentration and the temperature obtained by simulating the above case are almost similar to the research paper by M. Son. Hence the mesh was validated for the combustion analysis.

**Grid Independence Study** Grid independent analysis is done in order to evaluate the sizing of the components in order to construct the organized grid. The findings are strongly determined by the element distribution in a given domain. The iteration process is influenced by the distribution of components, so final converged values can vary. As a consequence, a grid independent analysis is needed to ensure that the result variables are independent of the number of components. This also saves time and memory during computation.

The following is the elements distribution algorithm that was used for grid independent studies:

$$\text{Number of elements required} = conv \sum (n \approx 2n \approx 4n \approx \dots \approx 2mn)$$

For each mesh that is evaluated, the number of elements is doubled. When meshing a structured mesh, however, the device domain controls the element distribution, so an exact number of elements cannot be obtained. However, since the element size and domain boundary distribution can be regulated, the number of elements can be counted to the nearest point. The control component and the tolerance relativistic element are two other significant features of the grid independent analysis. The tracking vector allows one to calculate the net difference in consecutive values and determine whether or not independency has been reached.

Setup Option	Unit Selected
Turbulence Model	k-epsilon(Standard)
Species Model	Species Transport
State Relation	Equilibrium Reaction
Convergence Criterion	10 <sup>-6</sup>

**Table 4.** Grid independent analysis parameters

Since the control variables can be conveniently updated to achieve the convergence condition, the traditional turbulence model was used. The k-epsilon norm was used, along with a non-premixed transport system in a chemical equilibrium state. Above is the final setup for the independence studies. As previously mentioned, choosing the right observation parameter is important for the mesh's independence. For the domain independent evaluation, two visualisation parameters of the total temperature of the domain were considered:

1. Maximum Total Temperature
2. Temperature distribution along the axial line of the domain

The grid independent simulation was carried out beginning from 40,000 elements and following the algorithm up to 200,000 elements and the results obtained are visualized in table below. It shows the distribution of the domain's overall total temperature and the number of nodes. The tolerance was important between mesh element sizes of 40,000 and 240,000, but as the mesh count increases, the relative variance decreases, and the distribution becomes linear after 169,695 components, meaning that the results are unaffected by the mesh count

adjustment.

Cases	Mesh Nodes (10 <sup>5</sup> )	Temperature (K)
Case 1	0.5	3345
	1	3280
	1.5	3270
	2	3273
	2.5	3277
Case 2	0.5	3296
	1	3250
	1.5	3233
	2	3240
	2.5	3241
Case 4	0.5	3345
	1	3280
	1.5	3233
	2	3270
	2.5	3273
Case 5	0.5	3347
	1	3279
	1.5	3265
	2	3277
	2.5	3275

**Table 5.** Mesh Independent Solution

### Propellant Optimization

Propellant optimization was carried out by using the open-source software name NASA Chemical Equilibrium and Application software (NASACEA). Different propellants are selected and then by using this software, o/f is selected and then thrust calculation is done for comparison. Performance parameters were obtained from software and thus these values are used in rocket thrust equations to calculate thrust.

The following combination of fuel-oxidizer were analyzed for the same, Methane (CH<sub>4</sub>) (L)-Oxygen(O<sub>2</sub>),

- Wax (C<sub>32</sub>H<sub>66</sub>)-Nitrous oxide(N<sub>2</sub>O)
- Hydrazine(N<sub>2</sub>H<sub>4</sub>)-Hydrogen peroxide(H<sub>2</sub>O<sub>2</sub>) Monomethyl
- Hydrazine (CH<sub>6</sub>N<sub>2</sub>)- dinitrogen Tetraoxide (N<sub>2</sub>O<sub>4</sub>)

After putting the necessary input values into the NASA CEA software, the performance parameters were noted and thrust was theoretically calculated using the rocket equations.

The initial pressure was choose to be 10bar with

the estimated chamber temperature to be 3800k. We have used thrust coefficient and chamber pressure from NASA CEA software output and calculated thrust using the following equation

$$C_f = \frac{T}{P_c A_t} \quad (1)$$

where,

$C_f$ - Thrust Coefficient

$T$  - Thrust

$P_c$  - Chamber Pressure

$A_t$  - Throat Area

SNo.	Propellant	Thrust(N)
1.	O <sub>2</sub> & CH <sub>4</sub>	128.74246
2.	N <sub>2</sub> O & C <sub>33</sub> H <sub>66</sub>	126.0721
3.	N <sub>2</sub> H <sub>4</sub> & H <sub>2</sub> O <sub>2</sub>	129.7477
4.	N <sub>2</sub> O <sub>4</sub> & CH <sub>6</sub> N <sub>2</sub>	128.4025

**Table 6.** Thrust Calculation of Propellants

Taking throat diameter to be 10mm. Table 5 shows the final values of thrust produced in newton (N), by each propellant combination.

### Result and Explanation

For the purpose of comparison and finding the optimum design, three parameters were considered: temperature, mass fraction of H<sub>2</sub>O and mass fraction of OH. Since H<sub>2</sub>O is the major product of combustion, a certain amount of its molar concentration indicates that the reaction is finished. Temperature parameter would indicate about the right temperature to be achieved after combustion process takes place which also helps in the thermal management of the chamber walls. Mass fraction of OH indicates at what point's reaction is high. As compared to the 20-degree pintle angle, the 50-degree pintle angled injectors have a steadier flow. When the recirculation areas are illuminated, they are far farther away from the pintle head, preventing unburned droplets from interfering with the incoming stream. However, in this situation, there is a fair risk that the droplets will not be charred when they leave the nozzle. As compared to the 20 degree pintle angle, this reduces combustion efficiency to a degree. However, it is fair to say that injectors with 50 degree pintle angles are less vulnerable to combustion instability than those with 20 degree pintle angles. As compared to the 20 degree pintle angle, the mass flow rates are lower. In terms of throttling range and maximum thrust

produced, the 50 degree pintle angle has the upper hand. In contrast to the 20 degree, the Lopen, max range limit is very high. By using a 20 degree pintle angle is that the recirculation region gets dangerously close to the pintle head. However, since the unburned particles are near to the incoming current, the particles migrate out of the surge, touching the hotspots and releasing energy at other antinodes. This will almost certainly trigger combustion instability.

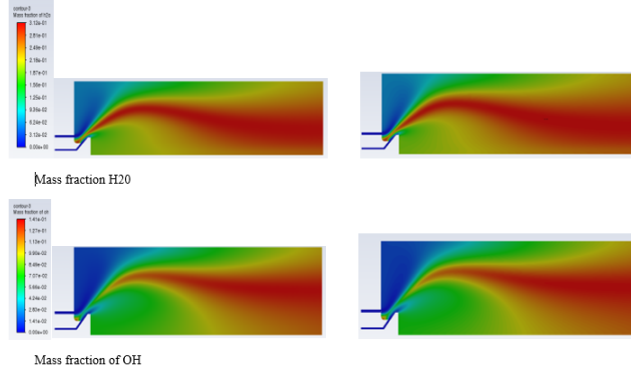


**Figure 6.** Numerical contours

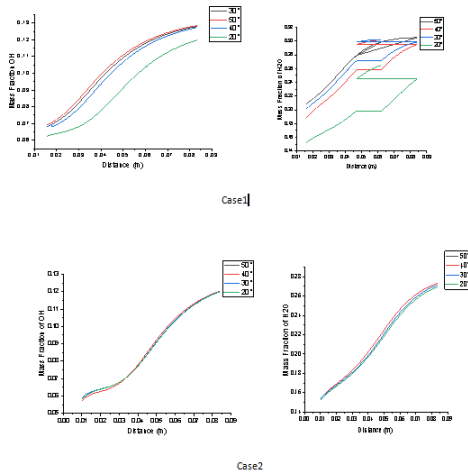


**Figure 7.** Mass fraction of OH and H2O a)Case1 B)Case2

## Conclusion

The primary goal of the analysis is to study the change in physics of combustion using two different geometries with varying pintle tip angle and centre post radius. Simulations are done using liquid Oxygen and methane to determine the effect of different geometries and recirculation zones to study combustion of pintle injectors. Various propellant combina-

tions are selected to study its properties using open source software to get the maximum value of thrust. From this analysis, result can be concluded as: High pintle angle shows better combustion performance and stable flow compared to smaller angles. Recirculation formed is away from pintle head in wider angles that does not allow unburnt particles to mix with incoming stream and keeps the particle within the flow preventing the formation of hotspots and combustion instability. By studying various propellant combinations, N<sub>2</sub>H<sub>4</sub>&H<sub>2</sub>O<sub>2</sub> is the best propellant combination that gives the maximum value of thrust when compared to other combinations.

## Acknowledgement

We would like to thank our mentor Gurunadh Velidi for his guidance and constant support. It was a privilege to work under him. We are thankful to the University of Petroleum and Energy Studies, for providing us the computational facilities to conduct our research. In the end, we would like to express our gratitude to our parents, family members without their support, this work would not have been possible.

## Nomenclature

$R$	radius
$L$	pintle opening distance
$Ea$	activation energy
$A$	pre-exponential factor
$B$	temperature exponent
$Ae$	exit area
$At$	throat area

## Subscripts

$cg$	center gap
$cp$	center post
$Pr$	pintle rod
$Pt$	pintle tip

## Greek Letters

$\rho$	density
$\sum$	summation

## References

- [1] Son, M., Radhakrishnan, K., Yoon, Y. and Koo, J., 2017. Numerical study on the combustion characteristics of a fuel-centered pintle injector for methane rocket engines. *Acta Astronautica*, 135, pp.139-149. <https://doi.org/10.1016/j.actaastro.2017.02.005>
- [2] Bedard, M., Feldman, T., Rettenmaier, A. and Anderson, W., 2012. Student design/build/test of a throttleable LOX-LCH<sub>4</sub> thrust chamber. In 48th AIAA/ASME/SAE/ASEE Joint

- Propulsion Conference & Exhibit (p. 3883).  
<https://doi.org/10.2514/6.2012-3883>
- [3] Son, M., Radhakrishnan, K., Koo, J., Kwon, O.C. and Kim, H.D., 2017. Design procedure of a movable pintle injector for liquid rocket engines. *Journal of propulsion and power*, 33(4), pp.858-869.<https://doi.org/10.2514/1.B36301>
- [4] Mahdavi, S.A., Ranjbar, A. and Farshchi, M., 2020. Effects of Dimensionless Numbers on the Pintle Injector Performance. *Modares Mechanical Engineering*, 20(7), pp.1761-1771.
- [5] Son, M., Yu, K., Radhakrishnan, K., Shin, B. and Koo, J., 2016. Verification on spray simulation of a pintle injector for liquid rocket engine. *Journal of thermal science*, 25(1), pp.90-96.  
<https://doi.org/10.1007/s11630-016-0838-y>
- [6] Casiano, M.J., Hulka, J.R. and Yang, V., 2010. Liquid-propellant rocket engine throttling: a comprehensive review. *Journal of propulsion and power*, 26(5), pp.897-923.  
<https://doi.org/10.2514/1.49791>
- [7] Frassoldati, A., Cuoci, A., Faravelli, T., Ranzi, E., Candusso, C. and Tolazzi, D., 2009, July. Simplified kinetic schemes for oxy-fuel combustion. In 1st International conference on sustainable fossil fuels for future energy (pp. 6-10).
- [8] Rajendran, R., Prasad, S., Subhashree, S., Phutane, T.S. and Saoor, V.S., DESIGN AND OPTIMIZATION OF PINTLE INJECTOR FOR LIQUID ROCKET ENGINE.
- [9] Huang, S.Y., Zhou, J., Liu, S.J. and Peng, H.Y., 2019. Effects of pintle injector on ethylene-air rocket-based continuous rotating detonation. *Acta Astronautica*, 164, pp.311-320.<https://doi.org/10.1016/j.actaastro.2019.08.019>
- [10] Jin, Xuan, Chibing Shen, Rui Zhou, and Xinxin Fang. "Effects of LOX Particle Diameter on Combustion Characteristics of a Gas-Liquid Pintle Rocket Engine." *International Journal of Aerospace Engineering* 2020 (2020). 2020.<https://doi.org/10.1155/2020/8867199>
- [11] Dressler, G., 2006, July. Summary of deep throttling rocket engines with emphasis on Apollo LMDE. In 42nd AIAA/ASME/SAE/ASEE Joint Propulsion Conference & Exhibit (p. 5220).<https://doi.org/10.2514/6.2006-5220>
- [12] Davis, L.A., 2016. First stage recovery. *Engineering*, 2(2), pp.152-153.
- [13] Sun, Z., Jia, Y. and Zhang, H., 2013. Technological advancements and promotion roles of Chang'e-3 lunar probe mission. *Science China Technological Sciences*, 56(11), pp.2702-2708.<https://doi.org/10.1007/s11431-013-5377-0>